Hybrid Precoding and Combining for Full-Duplex Millimeter Wave Communication

Joan Palacios[†], Javier Rodríguez-Fernández[‡], and Nuria González-Prelcic[‡§]

[†] IMDEA Networks, Email: joan.palacios@imdea.org

[‡] The University of Texas at Austin, Email: {javi.rf,ngprelcic}@utexas.edu

[§] Universidade de Vigo

Abstract—**Full-duplex (FD) communication is an enabling technology to increase spectral efficiency. The self-interference (SI) resulting from sharing time and frequency resources between different transceivers in FD mode must, however, be managed. At millimeter wave (mmWave) frequencies, FD communication is different than at sub-6 GHz frequencies, because non conventional MIMO architectures and large antenna arrays are often used. In this paper, we address a major challenge for FD mmWave systems: the design of hybrid precoders and combiners that simultaneously maximize the sum spectral efficiency and cancel the SI in the analog domain, to keep control of the signal level at the input of the analog-to-digital converters (ADCs). The optimal joint design is a very difficult problem, since it involves the optimization of eight precoding/combining matrices with several constraints, some of them non convex. We derive two suboptimal solutions which exhibit near-optimum spectral efficiency and significantly outperform prior work in terms of SI cancelation.**

I. INTRODUCTION

FD MIMO communication in sub-6 GHz bands has been actively studied in the last years due to its potential to double the spectral efficiency of a wireless system. A key ingredient of FD systems is the SI canceler. At lower frequencies, two main different solutions are available: based on analog-circuit domain methods plus digital cancelation of residual interference (see [1] for example), and based on spatial suppression using digital precoding/combining (such as in [2]).

The FD problem at mmWave bands is different, because the gain provided by large antenna arrays is needed and all-digital MIMO architectures are not feasible at every device. Hybrid MIMO architectures [3], with a digital and an analog precoding and combining stage, are supported in IEEE 802.11ay, and, to a limited extent, in the first release of 5G. In this context, spatial SI cancelation for FD is relevant—given the large number of antennas at the mmWave arrays, the number of degrees of freedom of the system is high, and the same analog precoding-combing circuit could be jointly used to beamform the communication signal and cancel the SI. This idea could also be applied to FD systems based on analog-only MIMO architectures. A few analog-only designs have been proposed in the recent literature [4], but these

architectures are less interesting because they are limited to single-stream communication.

To the best of our knowledge, only [5] derives a solution for a FD system based on a hybrid MIMO architecture operating at mmWave frequencies. The limitations of this design are, however, very strong. The SI is canceled in the digital domain, with the subsequent lack of control of the signal level at the input of the ADC, as we will show in our simulations. Moreover, the proposed method converges to eliminating paths and even communication in one direction.

In this paper, we propose a procedure to derive a solution for the design of a hybrid mmWave FD system that simultaneously cancels the SI in each radio frequency (RF) chain and significantly increases the spectral efficiency of the system. When compared to [5], we show that our method preserves the desired signal, while digital cancelation is not effective. Moreover, besides effectively cancelling SI, our design achieves a higher net spectral efficiency.

Notation: We use the following notation throughout this paper: x, $\mathbf{x}$, $\mathbf{X}$ are used for a scalar, a column vector and a matrix, respectively; $[]_a$, $[]_a$ denote a numerical and a categorical subindex; $[\mathbf{x}]_a$, $[\mathbf{X}]_{a,b}$, $[\mathbf{X}]_{:,b}$ are used for vector and matrix indexing; $\mathbf{X}^{1/2}$ represents the Cholesky decomposition of the symmetric positive semidefinite matrix $\mathbf{X}$, that s, $\mathbf{Q} = \mathbf{X}^{1/2}$ for $\mathbf{X} = \mathbf{Q}\mathbf{Q}^H$; $\mathbb{T}$ is the complex toroid $\{z \in \mathbb{C} \mid |z| = 1\}$; finally, $\|\mathbf{x}\|$ and $\|\mathbf{X}\|_F$ are the euclidean and Frobenius norm.

II. SYSTEM MODEL

We consider the narrowband hybrid FD mmWave communication system between transceivers i and j shown in Fig. 1, where variables i and j are reserved to denote the pairs $(i,j) \in \{(1,2),(2,1)\}$. Both transceivers operate in FD mode, so that they transmit and receive at the same time. The number of transmit and receive antennas at transceiver i is denoted as $N_{\text{Tx},i}$ and $N_{\text{Rx},i}$ respectively. Similarly, $N_{\text{RF-Tx},i}$ and $N_{\text{RF-Rx},i}$ represents the number of transmit and receive RF chains at transceiver i. $N_{\text{S},i}$ is the number of streams to be transmitted by transceiver i. The hybrid precoder at transceiver i is defined as $\mathbf{F}_i = \mathbf{F}_{\text{RF},i}\mathbf{F}_{\text{BB},i}$ with $\mathbf{F}_{\text{RF},i} \in \mathbb{T}^{N_{\text{Tx},i} \times N_{\text{RF-Tx},i}}$ and $\mathbf{F}_{\text{BB},i} \in \mathbb{C}^{N_{\text{RF-Tx},i} \times N_{\text{S},i}}$, while the hybrid combiner at transceiver j can be written as $\mathbf{W}_j = \mathbf{W}_{\text{RF},j}\mathbf{W}_{\text{BB},j}$, with $\mathbf{W}_{\text{RF},j} \in \mathbb{T}^{N_{\text{Rx},j} \times N_{\text{RF-Rx},j}}$ and $\mathbf{W}_{\text{BB},j} \in \mathbb{C}^{N_{\text{RF-Rx},j} \times N_{\text{S},i}}$.
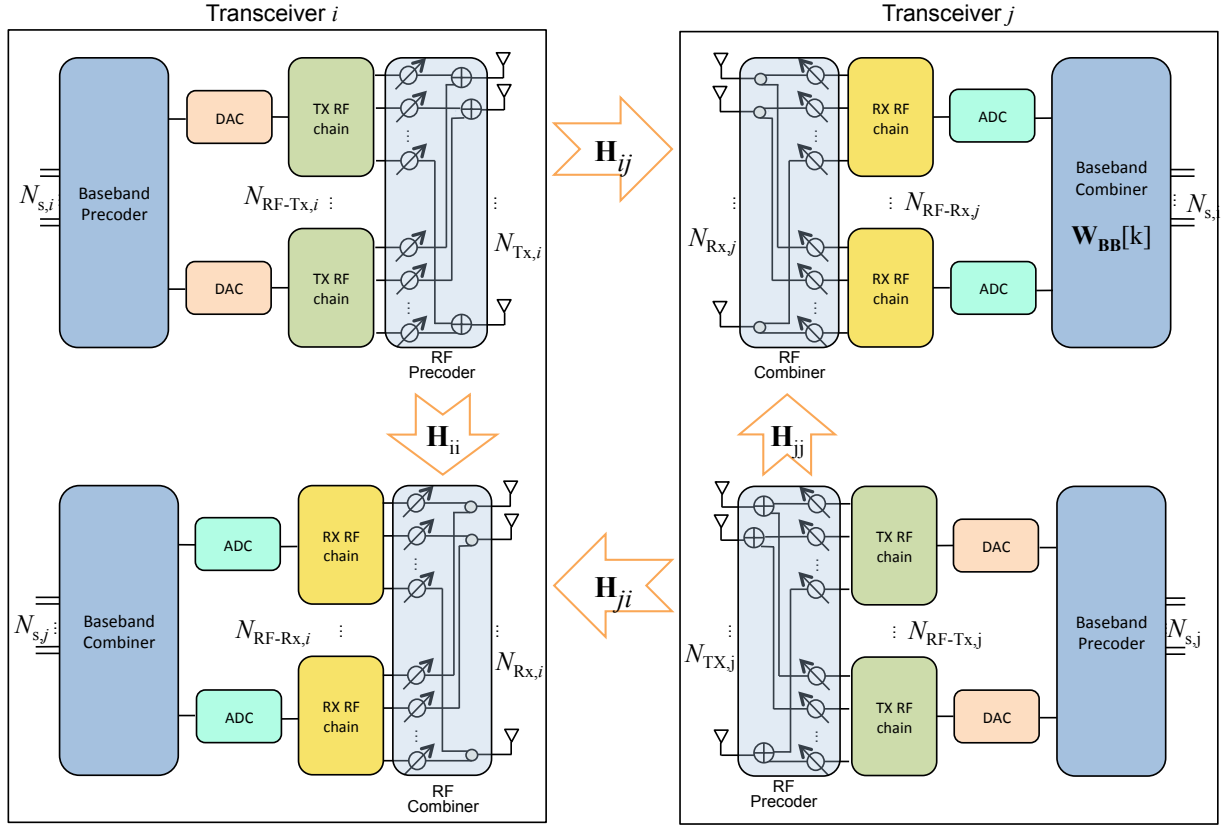
Fig. 1: Block diagram of the full duplex millimeter wave system based on a hybrid architecture.

We model the narrowband mmWave channel between the transmitter at node i and the receiver at node j as [3]

$$\mathbf{H}_{ij} = \sqrt{\frac{N_{\text{Tx},i}N_{\text{Rx},j}}{N_{\text{cl}}N_{\text{ray}}}} \sum_{c=1}^{N_{\text{cl}}} \sum_{\ell=1}^{N_{\text{ray}}} \beta_{c\ell,ij}\mathbf{a}_{\text{Rx},j}(\theta_{c\ell,i})\mathbf{a}_{\text{Tx},i}^{H}(\phi_{c\ell,i}),$$
(1)

where $\beta_{c,\ell}$ is the complex gain for the $\ell - th$ path in the $c - th$ cluster, $\mathbf{a}_{\text{Tx},i}(\phi_{c\ell,i})$ and $\mathbf{a}_{\text{Rx},j}(\theta_{c\ell,i})$ are the antenna array steering vectors at the transmitter and receiver evaluated at the azimuth angles of departure or arrival.

Assuming that the TX and RX arrays at each transceiver are close enough, the self-interference channels can be modeled with a line-of-sight nearfield model [4], [6]–[8]

$$[\mathbf{H}_{ii}]_{pq} = \frac{1}{d_{pq}^{(i)}}e^{-j2\pi\frac{d_{pq}^{(i)}}{\lambda}},$$
(2)

being $d_{pq}^{(i)}$ the distance between the p-th TX array and q-th RX array antennas both at transceiver i.

We define the average transmit power per symbol for the transmission between node i and node j as ρ_{ij}, the symbol transmitted by node i x_i with zero mean and unit variance, and the noise $\mathbf{n}_j$ at the receiver of node j is modeled as a zero-mean white Gaussian process with covariance $\sigma_j^2\boldsymbol{I}_{N_{Rx,j}}$. The general expression of the received signal at transceiver j for any precoder $\mathbf{F}_i$ and combiner $\mathbf{W}_j$ is

$$\mathbf{y}_j = \sqrt{\rho_{ij}}\mathbf{W}_j^H\mathbf{H}_{ij}\mathbf{F}_i\mathbf{x}_i + \sqrt{\rho_{jj}}\mathbf{W}_j^H\mathbf{H}_{jj}\mathbf{F}_j\mathbf{x}_j + \mathbf{W}_j^H\mathbf{n}_j, \quad (3)$$

where we can identify the desired component, the self-interference signal and the noise term.

III. HYBRID PRECODER AND COMBINER DESIGN FOR FULL DUPLEX SYSTEMS

In this section, our goal is to design hybrid precoders and combiners such that the spectral efficiency of the FD system is maximized, while the SI is canceled. First, we formulate the problem to be solved, and then, given its difficulty, we describe two strategies that provide a suboptimal solution. In Section IV, we evaluate the performance of our methods.

A. Problem formulation

To prevent ADCs saturation in the receive RF chains, the SI has to be canceled prior to the digital combiner, that is

$$\mathbf{W}_{\text{RF},j}^H\mathbf{H}_{jj}\mathbf{F}_j = \mathbf{0}.$$
(4)

Under canceled interference, expression in (3) becomes

$$\mathbf{y}_j = \sqrt{\rho_{ij}}\mathbf{W}_j^H\mathbf{H}_{ij}\mathbf{F}_i\mathbf{x}_i + \sigma_j\mathbf{W}_j^H\mathbf{n}_j,$$
(5)

and the spectral efficiency for the link between transceivers i and j can be computed as

$$\mathcal{R}_{ij} = \log_2\left(|\mathbf{I} + \mathbf{G}_{ij}\mathbf{G}_{ij}^H|\right),$$
$$\mathbf{G}_{ij} = \sqrt{\rho_{ij}}\mathbf{Q}_j^{-1}\mathbf{W}_j^H\mathbf{H}_{ij}\mathbf{F}_i, \quad \mathbf{Q}_j = (\sigma_j^2\mathbf{W}_j^H\mathbf{W}_j)^{1/2}.$$
(6)

If the interference is not canceled but can be assumed to be uncorrelated with the desired signal and unknown, we have to consider a different definition for $\mathbf{Q}_j$:

$$\mathbf{Q}_j = (\sigma_j^2 \mathbf{W}_j^H \mathbf{W}_j + \rho_{jj} \mathbf{W}_j^H \mathbf{H}_{jj} \mathbf{F}_j \mathbf{F}_j^H \mathbf{H}_{jj}^H \mathbf{W}_j)^{1/2}. \quad (7)$$

The sum spectral efficiency of the FD system can be written in this case as

$$\mathcal{R} = \log_2\left(|\mathbf{I} + \mathbf{G}_{12}\mathbf{G}_{12}^H|\right) + \log_2\left(|\mathbf{I} + \mathbf{G}_{21}\mathbf{G}_{21}^H|\right). \quad (8)$$

Assuming that the channels are known, the design problem for the full duplex setting can be stated as the maximization of $\mathcal{R}$ with respect to the precoder and combiner components, subject to the following constraints:

1) Zero forcing constraint at both transceivers to cancel SI.
2) Unit-norm hybrid precoders due to power limitation.
3) Unit-norm combing matrices, since $\mathcal{R}$ is invariant to scalings of the combiner.
4) Constant amplitude constraint due to the phase shifter-based implementation on the analog network.

This problem can be written in a mathematical way as

$$P1: \max_{\substack{\{\mathbf{F}_{\mathrm{RF},1}\},\{\mathbf{F}_{\mathrm{RF},2}\},\{\mathbf{F}_{\mathrm{BB},1}\},\{\mathbf{F}_{\mathrm{BB},2}\} \\ \{\mathbf{W}_{\mathrm{RF},1}\},\{\mathbf{W}_{\mathrm{RF},2}\},\{\mathbf{W}_{\mathrm{BB},1}\},\{\mathbf{W}_{\mathrm{BB},2}\}}} \log_2\left(|\mathbf{I} + \mathbf{G}_{12}\mathbf{G}_{12}^H|\right)$$
$$+ \log_2\left(|\mathbf{I} + \mathbf{G}_{21}\mathbf{G}_{21}^H|\right) \quad (9)$$

$$\text{s. t.} \quad \mathbf{W}_{\mathrm{RF},1}^H \mathbf{H}_{11} \mathbf{F}_1 = \mathbf{0}, \quad \mathbf{W}_{\mathrm{RF},2}^H \mathbf{H}_{22} \mathbf{F}_2 = \mathbf{0}, \quad (10)$$
$$\|\mathbf{F}_1\|_F = \|\mathbf{F}_2\|_F = \|\mathbf{W}_1\|_F = \|\mathbf{W}_2\|_F = 1, (11)$$
$$\mathbf{F}_{\mathrm{RF},1}, \mathbf{F}_{\mathrm{RF},2}, \mathbf{W}_{\mathrm{RF},1}, \mathbf{W}_{\mathrm{RF},2} \in \mathbb{T}^{a \times b}. \quad (12)$$

where $a \times b$ is the matrix dimension corresponding to the number of antennas times the number of RF-chains. Defining $L_{ij} = \min(N_{\mathrm{RF\text{-}Tx},i}, N_{\mathrm{RF\text{-}Rx},j})$, we can compute an upper bound $\mathcal{R}^{\mathrm{UB}}$ to $\mathcal{R}$ in (8) by neglecting the self-interference and the CA constraints:

$$\mathcal{R}^{\mathrm{UB}} = \sum_{l=1}^{L_{12}} \log_2(1 + \lambda_{12}^{(l)} p_{12}^{(l)}) + \sum_{l=1}^{L_{21}} \log_2(1 + \lambda_{21}^{(l)} p_{21}^{(l)}), \quad (13)$$

with $\{\lambda_{ij}^{(l)}\}_{l \leq L_{ij}}$ being the squared strongest singular values of $\frac{\sqrt{\rho_{ij}}}{\sigma_j} \mathbf{H}_{ij}$ and $\{p_{ij}^{(l)}\}_{l \leq L_{ij}}$ their corresponding power allocation values by water filling. This expression can not be achieved, but it will be used as a benchmark for analysis.

B. Proposed strategy

The optimal design as formulated in $P1$ is a difficult problem, since it requires the optimization of eight matrices under non-convex constraints. The design of hybrid precoders and combiners has not even been solved yet for a half duplex setting, where condition (4) can be ignored and the design of both links is decoupled. In this section, we propose a suboptimal approach that handles the coupling between both directions of communication in a smart way, incorporating the zero SI constraint.

Our proposed strategy relies on finding first the most critical of the eight elements of the design, which are the analog
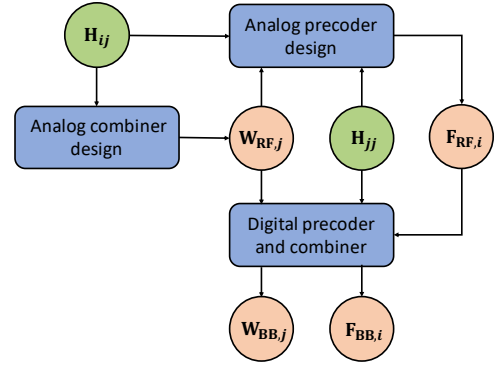

Fig. 2: Block diagram of the algorithm for the design of the eight precoders and combiners for duplex communication. Green and orange circles represent input parameters and variables to be designed, respectively. Notice that the algorithm requires both pairs $(i,j) = (1,2),(2,1)$ to enter the algorithm.

counterparts, since they are constrained to have module one entries. Then, we find the optimal digital filters that maximize the sum spectral efficiency and cancel the interference for the previously obtained analog stage.

For the design of the analog stage itself, we follow the same philosophy, and start by designing first the most critical elements. In this case, these are the analog combiners, since unlike the analog precoders, they cannot make use of their digital counterparts to cancel the interference.

In summary, the final procedure will consist of the following stages: 1) design of the analog combiners for both links; 2) joint design of the analog precoders; and 3) design of their digital counterparts. The flow of the algorithm is depicted in Fig. 2. Notice that both pairs of indices are computed in parallel, so when computing $\mathbf{F}_{\mathrm{RF},i}$, $\mathbf{W}_{\mathrm{RF},i}$ is available.

C. Analog combiners design

To design the analog combiner, we assume that the hybrid precoder will cancel the SI. Then, we rely on two well known approaches [9], [10] as a basis for this design as described below.

1) SVD-based approach (SVD): We consider the optimal design of a fully digital combiner based on the left singular vectors of the singular value decomposition (SVD) of the channel [9]. We also take into account that any fully digital combining matrix for N_{S} receive streams can be optimally synthesized with a hybrid structure when $N_{\mathrm{RF\text{-}Rx}} \geq 2N_{\mathrm{S}}$ [11].

With these two considerations, it is clear that we can optimally solve the digital problem for $N_{\mathrm{S}} = N_{\mathrm{RF\text{-}Rx}}/2$ and obtain $\mathbf{W}_j$. This solution is given by
$[\mathbf{W}_{\mathrm{RF},j}]_{a,b} = e^{\arccos(\frac{|[\mathbf{W}_j]_{a,b}|}{\max_{\bar{a}} |[\mathbf{W}_j]_{\bar{a},b}|})i}$, $[\mathbf{W}_{\mathrm{RF},j}]_{a,b+N_{\mathrm{S}}} = e^{-\arccos(\frac{|[\mathbf{W}_j]_{a,b}|}{\max_{\bar{a}} |[\mathbf{W}_j]_{\bar{a},b}|})i}$ The steps of the analog combiner design for the SVD-based method are described in Algorithm 1.

Algorithm 1 $\mathbf{W}_{\mathrm{RF},j}$ design based on the SVD

1: INPUT: $\mathbf{H}_{ij}$, $N_{\mathrm{RF\ Rx},j}$
2: Compute $\mathbf{U}$ as the left handed singular vectors of $\mathbf{H}_{ij}$.
3: Compute $\mathbf{W}_{\mathrm{RF},j}$ as the optimal approach to $[\mathbf{U}]_{:,1:N_{\mathrm{RF\ Rx},j}/2}$ described in [11]

2) Path beamforming (PB): This approach consists on physically directing the power radiated in the channel paths direction as described in [10].

First we need to decompose the communication channel into $N_{\mathrm{S}} = N_{\mathrm{RF\text{-}Rx},j}$ paths, that is

$$\mathbf{H}_{ij} \simeq \sqrt{\frac{N_{\mathrm{Tx},i}N_{\mathrm{Rx},j}}{N_{\mathrm{S}}}} \sum_{l}^{N_{\mathrm{S}}} \beta_{l,ij}\mathbf{a}_{\mathrm{Rx},j}(\theta_{l,j})\mathbf{a}_{\mathrm{Tx},i}^{H}(\phi_{l,i}).$$

We apply the sparse approximation algorithm in [12] to obtain this channel decomposition. With this strategy, the analog combiner is $W_{\mathrm{RF},j} = \mathbf{A}_{\mathrm{Rx}} = [\mathbf{a}_{\mathrm{Rx}}(\theta_{l,1}), \ldots, \mathbf{a}_{\mathrm{Rx}}(\theta_{l,N_{\mathrm{RF\text{-}Rx},j}})]$. The PB method is depicted in algorithm 2.

Algorithm 2 $\mathbf{W}_{\mathrm{RF},j}$ design by path skeleton

1: INPUT: $\mathbf{H}_{ij}$, $N_{\mathrm{RF\ Rx},j}$
2: Compute $\mathbf{A}_{\mathrm{Rx}}$ using channel decomposition in [12]
3: $\mathbf{W}_{\mathrm{RF},j} \leftarrow \mathbf{A}_{\mathrm{Rx}}$

D. Analog precoders design

The design of the analog precoders must take into account the SI cancellation constraint in (4). With a fixed analog combiner $\mathbf{W}_{\mathrm{RF},i}$, this expression means that every column of the precoder $\mathbf{F}_i$ is in the kernel of $\mathbf{H}_{ii}^{H}\mathbf{W}_{\mathrm{RF},i}\mathbf{W}_{\mathrm{RF},i}\mathbf{H}_{ii}$. Thus, it can be expressed as $\mathbf{Y}_i\hat{\mathbf{F}}_i$ for $\mathbf{Y}_i$ a base of the kernel. Considering $\hat{\mathbf{F}}_i$ as a new variable, the problem boils down to finding the optimal precoder for the scenario without interference defined by

$$P2: \quad \max \log_2(\mathbf{I} + \mathbf{G}_{ij}\mathbf{G}_{ij}^{H}) \tag{14}$$

with $\mathbf{G}_{ij} = \frac{\sqrt{\rho_{ij}}}{\sigma_j}(\mathbf{W}_{\mathrm{RF},j}^{H}\mathbf{W}_{\mathrm{RF},j})^{-\frac{1}{2}}\mathbf{W}_{\mathrm{RF},j}^{H}\mathbf{H}_{ij}\mathbf{Y}_i\hat{\mathbf{F}}_i$.

The solution to $P2$ is $\hat{\mathbf{F}}_i$ comprising of the N_{S} strongest right singular vectors of $(\mathbf{W}_{\mathrm{RF},j}^{H}\mathbf{W}_{\mathrm{RF},j})^{-\frac{1}{2}}\mathbf{W}_{\mathrm{RF},j}^{H}\mathbf{H}_{ij}\mathbf{Y}_i$, with additional power allocation as described in [13]. Accordingly, the precoder can be retrieved as $\mathbf{F}_i = \mathbf{Y}_i\hat{\mathbf{F}}_i$. Notice that so far, the constraint of $\mathbf{F}_i$ being a feasible hybrid precoder has not been considered. This is owing to the fact that such constraint becomes very complex when applied to $\hat{\mathbf{F}}_i$. To circumvent this issue, we will optimally approach digitally generated beam-patterns by setting $N_{\mathrm{S}} = N_{\mathrm{RF\text{-}Tx},i}/2$ and finding the optimal analog precoder $\mathbf{F}_{\mathrm{RF},i}$ that approximates the all digital one This provides us with an analog precoder that ensures the existence of a good solution to the final problem. Notice, however, that although this algorithm provides a feasible digital precoder, we will only consider the solution to compute $\mathbf{F}_{\mathrm{RF},1}$ and $\mathbf{F}_{\mathrm{RF},2}$.

E. Digital combiners and precoders design

In this section, we derive the expression of the optimal digital precoders and combiners, that is, that maximize the sum spectral efficiency in (6) and cancel the interference, for a given choice of their analog counterparts.

The digital precoder can be written as $\mathbf{F}_{\mathrm{BB},i} = \mathbf{X}_i\hat{\mathbf{F}}_{\mathrm{BB},i}$, for $\mathbf{X}_i$ a base of the kernel of $\mathbf{F}_{\mathrm{RF},i}^{H}\mathbf{H}_{ii}^{H}\mathbf{W}_{\mathrm{RF},i}^{H}\mathbf{W}_{\mathrm{RF},i}\mathbf{H}_{ii}\mathbf{F}_{\mathrm{RF},i}$, and $\hat{\mathbf{F}}_{\mathrm{BB},i}$ the new variable to be optimized. Taking this into account, $\mathbf{G}_{ij}$ in (6) can be written as

$$\mathbf{G}_{ij} = \mathbf{Q}_j^{-1}\mathbf{W}_{\mathrm{BB},j}^{H}\mathbf{W}_{\mathrm{RF},j}^{H}\mathbf{H}_{ij}\mathbf{F}_{\mathrm{RF},i}\mathbf{X}_i\tilde{\mathbf{F}}_{\mathrm{BB},i}. \tag{15}$$

Now, we can decompose the terms and rearrange them to define new variables that help us solve the problem of designing the digital precoders and combiners. For this purpose, let us consider the following singular value decompositions

$$\mathbf{W}_{\mathrm{RF},j} = \mathbf{U}_{\mathrm{W},j}\mathbf{S}_{\mathrm{W},j}\mathbf{V}_{\mathrm{W},j}^{H}, \quad \mathbf{F}_{\mathrm{RF},i}\mathbf{X} = \mathbf{U}_{\mathrm{F},i}\mathbf{S}_{\mathrm{F},i}\mathbf{V}_{\mathrm{F},i}^{H},$$

such that we can define $\hat{\mathbf{H}}_{ij} = \mathbf{U}_{\mathrm{W},j}^{H}\mathbf{H}\mathbf{U}_{\mathrm{F},i}$, $\hat{\mathbf{W}}_j = \mathbf{S}_{\mathrm{W},j}\mathbf{V}_{\mathrm{W},j}^{H}\mathbf{W}_{\mathrm{BB},j}$, and $\hat{\mathbf{F}}_i = \mathbf{S}_{\mathrm{F},i}\mathbf{V}_{\mathrm{F},i}^{H}\tilde{\mathbf{F}}_{\mathrm{BB},i}$. With these new variables, the problem is redefined as

$$\mathbf{G}_{ij} = \mathbf{Q}_j^{-1}\hat{\mathbf{W}}_j^{H}\hat{\mathbf{H}}_{ij}\hat{\mathbf{F}}_i, \tag{16}$$

in which, due to orthonormality of the matrices $\mathbf{U}_{\mathrm{W},j}$ and $\mathbf{U}_{\mathrm{F},i}$, the following constrains are equivalent to the original ones

$$\begin{aligned} \mathbf{W}_j^{H}\mathbf{W}_j &= \hat{\mathbf{W}}_j^{H}\mathbf{U}_{\mathrm{W},j}^{H}\mathbf{U}_{\mathrm{W},j}\hat{\mathbf{W}}_j = \hat{\mathbf{W}}_j^{H}\hat{\mathbf{W}}_j = \mathbf{Q}\mathbf{Q}^{H}/\sigma_j^2, \\ \|\mathbf{W}_j\| &= \|\mathbf{U}_{\mathrm{W},j}\hat{\mathbf{W}}_j\| = \|\hat{\mathbf{W}}_j\| = 1, \\ \|\mathbf{F}_i\| &= \|\mathbf{U}_{\mathrm{F},i}\hat{\mathbf{F}}_i\| = \|\hat{\mathbf{F}}_i\| = 1. \end{aligned} \tag{17}$$

This is equivalent to the rate maximization problem without the interference cancellation, so we can solve it as $\hat{\mathbf{W}}_j = [\mathbf{U}_{ij}]_{:,1:N}$, $\hat{\mathbf{F}}_i = [\mathbf{V}_{ij}]_{:,1:N}\mathbf{D}$, for the singular value decomposition $\hat{\mathbf{H}}_{ij} = \mathbf{U}_{ij}\mathbf{S}_{ij}\mathbf{V}_{ij}^{H}$ and $\mathbf{D}$ the diagonal matrix containing the power allocation coefficients, obtained by the standard water-filling algorithm to the diagonal of matrix $\frac{\rho_{ij}}{\sigma_j^2}[\mathbf{S}_{ij}^2]_{1:N,1:N}$. Taking into account the considered definitions and transformations, the final solution is retrieved as

$$\begin{aligned} \mathbf{W}_{\mathrm{BB},j} &= \mathbf{V}_{\mathrm{W},j}\mathbf{S}_{\mathrm{W},j}^{-1}[\mathbf{U}_{ij}]_{:,1:N} \\ \mathbf{F}_{\mathrm{BB},i} &= \mathbf{X}_i\mathbf{V}_{\mathrm{F},i}\mathbf{S}_{\mathrm{F},i}^{-1}[\mathbf{V}_{ij}]_{:,1:N}\mathbf{D} \end{aligned} \tag{18}$$

With this, we have the last piece of our puzzle to solve the full-duplex communication problem, and thus the solution to the problem is complete.

IV. RESULTS

In this section, we present numerical results on the performance of our proposed hybrid precoding and combining algorithms for full duplex millimeter wave systems. The considered performance metrics are the sum spectral efficiency defined in (8), and the expectation of the maximum interference, defined as

$$mI = mI_1 + mI_2, \tag{19}$$

with mI_j the maximum interference-to-noise-ratio experienced at the output of an RF chain (prior to the ADC)

$$mI_j = \max_k \frac{\rho_{jj}}{\sigma_j^2} \|[\mathbf{W}_{\text{RF},j}]_{:,k}^H \mathbf{H}_{jj} \mathbf{F}_j\|^2. \qquad (20)$$

A FD design algorithm leading to a high value for this metric could not be used in practise, since the signal we want to decode would be destroyed. As a reference for the obtained sum spectral efficiency, we compare against its loose bound $\mathcal{R}^{\text{UB}}$ defined in (13). In addition to these performance metrics we also measure the computation time of each method.

In our simulation setup, we consider that both transmitter and receiver per device use $N_{\text{Tx},\ell} = N_{\text{Rx},\ell} = 64$ antennas, $\ell = 1, 2$. To simplify the analysis on the number of RF chains used for transmission and reception, we assume that both devices have the same RF-chain structure, this is $N_{\text{RF, Rx, 1}} = N_{\text{RF, Rx, 2}} = N_{\text{RF, Rx}}$ and $N_{\text{RF, Tx, 1}} = N_{\text{RF, Tx, 2}} = N_{\text{RF, Tx}}$. The performance evaluation of our methods is accomplished through Monte-Carlo simulation, averaging the results for 1024 different channel realizations.

To generate the MIMO communication channels $\mathbf{H}_{ij}$, we use QuaDRiGa channel simulator [14] for the 3GPP TR 38.901 UMa scenario, considering a Rician factor of -10 dB corresponding to a NLOS setting, a sampling time of 0.509 ns as in the 5G New Radio (5G-NR) wireless standard [15], and a single OFDM sub-carrier, as we are considering a narrow-band model. The SI channels are generated from the LoS near field channel model with $\rho_{jj}/\sigma_j^2 = 30dB$.

We evaluate first the effectiveness of our two approaches (HFD-SVD, and HFD-PB) to cancel SI, and compare to the results provided by the method described in [5], that we denote as HFD. Fig. 3 invalidates the design described in [5] as expected, since it has been derived under the erroneous assumption that the digital combiner can be used to cancel the SI. The received interference for HFD-SVD and HFD-PB is zero. The curve for HFD shows that the received interference strength in the analog domain is three orders of magnitude larger than the noise power. Consequently, the useful signal experiences really high interference, what makes it impossible to retrieve it in the digital domain. Even after showing that this method does not properly cancel the interference, we will still use it in the rest of this section as a benchmark for our methods.

In the next figures we analyze the sum spectral efficiency of the different methods when operating with different numbers of RF chains for transmission and reception, ranging from 1 to 18, and different SNR values $\frac{\rho_{12}}{\sigma_2^2} = \frac{\rho_{21}}{\sigma_1^2}$, ranging from -30 dB to 10 dB. We also compare the performance of our methods to $\mathcal{R}^{\text{UB}}$, the upper-bound in (13) obtained when there is no SI. The purpose of this simulation is three-fold: i) it allows deciding which is the most suitable hybrid precoding and combining strategy under different SNRs, ii) learning how to distribute RF-chains for transmission/reception, and iii) understand how the number of RF-chains affects the communication performance.

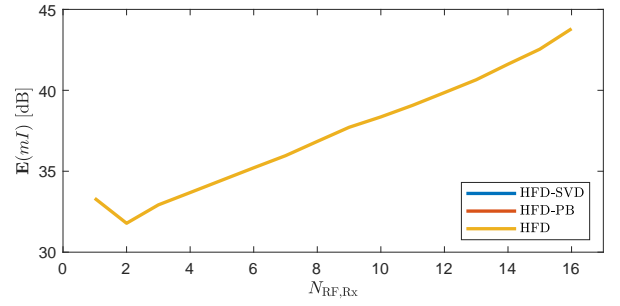Fig. 4 shows the Spectral Efficiency evolution as we

Fig. 3: Analog Interference as a function of $N_{\text{RF-Rx}}$ when $N_{\text{RF-Tx}} + N_{\text{RF-Rx}} = 18$.
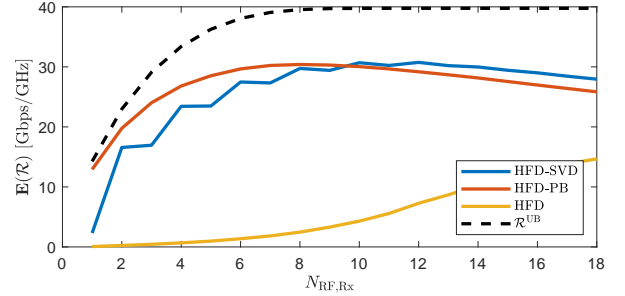

Fig. 4: Spectral Efficiency Sum as a function of $N_{\text{RF-Rx}}$ when $N_{\text{RF-Tx}} = 18$ and $\frac{\rho_8}{\sigma_2^2} = \frac{\rho_{21}}{\sigma_1^2} = -10dB$.

increase the number of RF-chains for reception with an SNR of -10 dB and a large number of RF-chains for transmission (12), such that the flexibility in the transmitter is high enough. Consequently, only the effects of the parameters in the receiver are analyzed. Besides completely canceling the SI, as shown before, our methods also significantly outperform HFD in [5] in terms of sum spectral efficiency. The main effect we observe in this figure is that the sum spectral efficiency is not monotonically increasing with the number of RF chains, contrary to the scenario without SI. Another effect is the parity behavior (zig-zag) in the HBF-SVD method, due to the fact that this strategy only uses an even number of RF chains, discarding the ones not being used.

One of our goals is to understand how to make use of the available RF-chains, that is, is deciding how many RF-chains
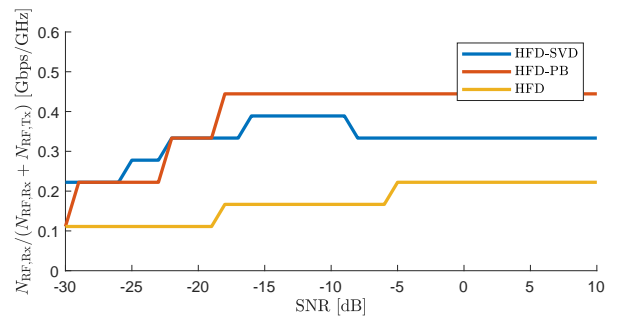

Fig. 5: Optimal $N_{\text{RF-Tx}}, N_{\text{RF-Rx}}$ allocation over SNR for $N_{\text{RF-Tx}} + N_{\text{RF-Rx}} = 18$
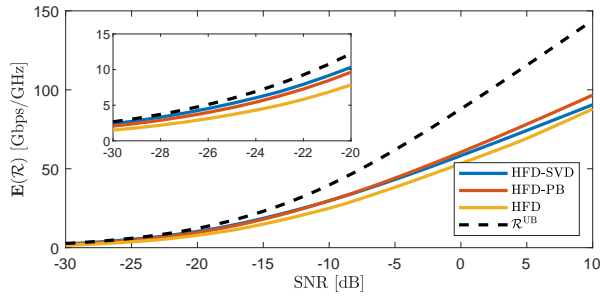
Fig. 6: Spectral Efficiency Sum with $N_{\text{RF-Tx}}, N_{\text{RF-Rx}}$ allocation as a function of the SNR for $N_{\text{RF-Tx}} + N_{\text{RF-Rx}} = 18$.
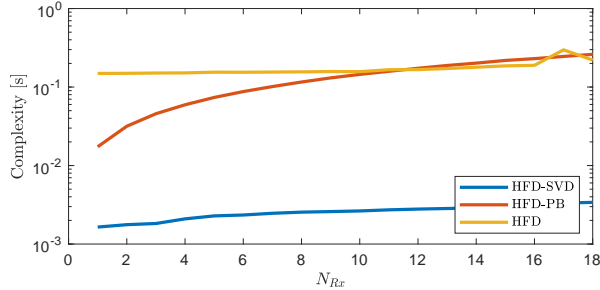

Fig. 7: Computational time as a function of $N_{\text{RF-Rx}}$ when $N_{\text{RF-Tx}} = 18$ and $\frac{\rho_8}{\sigma_2^2} = \frac{\rho_{21}}{\sigma_1^2} = -10 dB$.

to use for transmission and reception. We study in Fig. 5 how the optimal RF-chain allocation ($N_{\text{RF-Tx}}/(N_{\text{RF-Tx}} + N_{\text{RF-Rx}})$) in terms of maximizing $\mathcal{R}$, evolves with the SNR when the number of total RF chains in the link is fixed. As the SNR increases, a larger number of multipath components in the channel is used, thereby resulting in higher sum spectral efficiency for a greater number of RF-chains for reception. This behavior stops at a ratio of one third for the HFD-PB method, due to the fact that each transceiver uses one RF-chain for reception and two for transmission per path. For the HFD-SVD method, this behavior stops for a ratio slightly smaller than $1/2$, since this algorithm attempts to use two RF-chains, both for reception and transmission, per singular value of the channel matrix decomposition.

After studying the RF-chain allocation problem, we pick the RF-chain configuration maximizing the average sum spectral efficiency $\mathcal{R}$ for every SNR value and see how $\mathcal{R}$ varies in Fig. 6. At high SNR, a larger number of multipath components become relevant for communication, while at low SNR the power allocation per path is focused on the strongest ones. For this reason, the HFD-PB method outperforms its HFD-SVD counterpart at high SNR regime, while the HFD-SVD method outperforms its HFD-PB counterpart at low SNR regime.

As for the computational time, the average time it takes to complete each algorithm is depicted in figure 7. Since the maximum number of $N_{\text{RF-Rx}}$ used by any algorithm is lower than 9 for the selected number of RF-chains, $N_{\text{RF-Tx}} + N_{\text{RF-Rx}} = 18$, both HFD-SVD and HFD-PB outperform HFD.

V. CONCLUSIONS

In this paper we proposed the first design for hybrid precoders and combiners to operate in a full duplex millimeter wave system that effectively cancels the SI while providing near optimal sum spectral efficiency values. We also showed that our designs significantly outperforms the only previously proposed design for this problem, which clearly fails to cancel the SI present at the ADC input signals.

REFERENCES

[1] M. Heino, D. Korpi, T. Huusari, E. Antonio-Rodriguez, S. Venkatasub-ramanian, T. Riihonen, L. Anttila, C. Icheln, K. Haneda, R. Wichman, and M. Valkama, "Recent advances in antenna design and interference cancellation algorithms for in-band full duplex relays," *IEEE Communications Magazine*, vol. 53, no. 5, pp. 91–101, May 2015.

[2] E. Everett, C. Shepard, L. Zhong, and A. Sabharwal, "SoftNull: Many-Antenna Full-Duplex Wireless via Digital Beamforming," *IEEE Transactions on Wireless Communications*, vol. 15, no. 12, pp. 8077–8092, Dec 2016.

[3] R. W. Heath, N. Gonzlez-Prelcic, S. Rangan, W. Roh, and A. M. Sayeed, "An Overview of Signal Processing Techniques for Millimeter Wave MIMO Systems," *IEEE Journal of Selected Topics in Signal Processing*, vol. 10, no. 3, pp. 436–453, April 2016.

[4] X. Liu, Z. Xiao, L. Bai, J. Choi, P. Xia, and X.-G. Xia, "Beamforming based full-duplex for millimeter-wave communication," *Sensors*, vol. 16, no. 7, p. 1130, Jul 2016.

[5] K. Satyanarayana, M. El-Hajjar, P. Kuo, A. Mourad, and L. Hanzo, "Hybrid beamforming design for full-duplex millimeter wave communication," *IEEE Transactions on Vehicular Technology*, vol. 68, no. 2, pp. 1394–1404, Feb 2019.

[6] L. Li, K. Josiam, and R. Taori, "Feasibility study on full-duplex wireless millimeter-wave systems," in *2014 IEEE International Conference on Acoustics, Speech and Signal Processing (ICASSP)*, May 2014, pp. 2769–2773.

[7] S. Rajagopal, R. Taori, and S. Abu-Surra, "Self-interference mitigation for in-band mmWave wireless backhaul," in *2014 IEEE 11th Consumer Communications and Networking Conference (CCNC)*, Jan 2014, pp. 551–556.

[8] Z. Xiao, P. Xia, and X. Xia, "Full-Duplex Millimeter-Wave Communication," *IEEE Wireless Communications*, vol. 24, no. 6, pp. 136–143, Dec 2017.

[9] O. El Ayach, R. W. Heath, S. Abu-Surra, S. Rajagopal, and Z. Pi, "The capacity optimality of beam steering in large millimeter wave MIMO systems," in *2012 IEEE 13th International Workshop on Signal Processing Advances in Wireless Communications (SPAWC)*. IEEE, 2012, pp. 100–104.

[10] J. Palacios, D. De Donno, and J. Widmer, "Tracking mm-Wave channel dynamics: Fast beam training strategies under mobility," in *IEEE INFOCOM 2017-IEEE Conference on Computer Communications*. IEEE, 2017, pp. 1–9.

[11] F. Sohrabi and W. Yu, "Hybrid digital and analog beamforming design for large-scale MIMO systems," in *2015 IEEE International Conference on Acoustics, Speech and Signal Processing (ICASSP)*. IEEE, 2015, pp. 2929–2933.

[12] Y. C. Pati, R. Rezaiifar, and P. S. Krishnaprasad, "Orthogonal matching pursuit: recursive function approximation with applications to wavelet decomposition," in *Proceedings of 27th Asilomar Conference on Signals, Systems and Computers*, Nov 1993, pp. 40–44 vol.1.

[13] R. Mndez-Rial, C. Rusu, N. Gonzlez-Prelcic, and R. W. Heath, "Dictionary-free hybrid precoders and combiners for mmWave MIMO systems," in *2015 IEEE 16th International Workshop on Signal Processing Advances in Wireless Communications (SPAWC)*, June 2015, pp. 151–155.

[14] S. Jaeckel, L. Raschkowski, K. Brner, and L. Thiele, "QuaDRiGa: A 3-D Multi-Cell Channel Model With Time Evolution for Enabling Virtual Field Trials," *IEEE Transactions on Antennas and Propagation*, vol. 62, no. 6, pp. 3242–3256, June 2014.

[15] 3GPP, "Technical specification group radio access network: Physical channels and modulation (release 15)," March 2018.